

Nowcasting with mixed frequency data using Gaussian processes

Niko HAUZENBERGER

University of Strathclyde, United Kingdom

Massimiliano MARCELLINO

Bocconi University, IGIER, Baffi, Bidsa, CEPR, Italy

Michael PFARRHOFER

WU Vienna, Austria

Anna STELZER

Oesterreichische Nationalbank, Austria

Draft version

February 16, 2024

We propose and discuss Bayesian machine learning methods for mixed data sampling (MIDAS) regressions. This involves handling frequency mismatches with restricted and unrestricted MIDAS variants and specifying functional relationships between many predictors and the dependent variable. We use Gaussian processes (GP) and Bayesian additive regression trees (BART) as flexible extensions to linear penalized estimation. In a nowcasting and forecasting exercise we focus on quarterly US output growth and inflation in the GDP deflator. The new models leverage macroeconomic Big Data in a computationally efficient way and offer gains in predictive accuracy along several dimensions.

JEL: C11, C22, C53, E31, E37

KEYWORDS: predictive regression, forecasting, MIDAS, regression trees

Contact: Michael Pfarrhofer (michael.pfarrhofer@wu.ac.at), Department of Economics, WU Vienna University of Economics and Business. The views expressed in this paper are those of the authors and do not necessarily reflect the views of the Oesterreichische Nationalbank or the Eurosystem. Pfarrhofer acknowledges funding by the Jubiläumsfonds of the Oesterreichische Nationalbank, grant no. 18765.

1. INTRODUCTION

This paper develops flexible nowcasting and forecasting methods by combining elements from three strands of econometric literature. *First*, drawing from the mixed data sampling (MIDAS) framework introduced by [Ghysels *et al.* \(2007\)](#), see also [Andreou *et al.* \(2010\)](#), [Ghysels \(2016\)](#), or [Ghysels *et al.* \(2024\)](#) for a recent review, we leverage techniques that permit the efficient use of predictors sampled at a higher frequency than the target variable. *Second*, the Big Data literature, based on the idea that using a large set of predictors combined with penalized estimators or Bayesian shrinkage can improve predictive accuracy, see e.g., [Babii *et al.* \(2022\)](#) and [Mogliani and Simoni \(2021\)](#) in the context of mixed frequency models. *Third*, the machine learning literature, which postulates that proper algorithms combined with computing power can uncover complicated relationships among variables (economic and financial ones, in our case) and hence improve predictions, see e.g., [Hastie *et al.* \(2009\)](#).

Our baseline framework uses Gaussian Processes (GPs) to estimate the unknown and perhaps nonlinear relationships between a target variable and a large set of mixed frequency predictors nonparametrically. GPs have been used previously in single frequency economic applications, see e.g., [Clark *et al.* \(2024a\)](#) in the context of inflation forecasting, or [Hauzenberger *et al.* \(2024\)](#) who estimate nonlinear effects of uncertainty shocks. By contrast, to handle mixed frequencies in this nonlinear context, we use several variants of restricted MIDAS polynomials in the spirit of [Ghysels *et al.* \(2007\)](#), or the unrestricted MIDAS (U-MIDAS) approach of [Foroni *et al.* \(2015\)](#), where each single high frequency predictor is split into many low frequency ones.

As a nonparametric alternative to GPs for modeling the conditional expectation of the dependent variable in MIDAS models, we consider Bayesian Additive Regression Tree (BART, originally proposed by [Chipman *et al.*, 2010](#)) models. While GPs estimate nonlinear functions via a (theoretically infinite) mixture of Gaussian distributions, BART does so by means of a sum of regression trees, which can be considered as generalizations of step functions. BART has been shown to perform quite well for nowcasting and forecasting with time series data in macroeconomic applications (see, e.g., [Clark *et al.*, 2023; 2024b; Huber *et al.*, 2023](#)).¹

To gauge the role of nonlinearities of an unknown form, we benchmark our nonparametric extensions to their linear counterparts. These are equipped with global-local shrinkage

¹ A recent review and discussion of GPs and BART in a (multivariate) time series context is provided in [Marcellino and Pfarrhofer \(2024\)](#).

priors and reflect the recent (Bayesian) literature in the MIDAS context (see also [Rodriguez and Puggioni, 2010](#); [Mogliani and Simoni, 2021](#)). Besides, we implement all competing model specifications with and without stochastic volatility (SV) in the error terms, as SV has been shown as important for improving short-horizon density forecasts in previous work based on linear mixed frequency models (see, e.g., [Carriero *et al.*, 2015; 2022](#)).

We develop efficient Bayesian estimation algorithms based on Markov chain Monte Carlo (MCMC) sampling, which permit to use very large sets of predictors to produce point, density and tail forecasts in a computationally efficient manner.² The resulting model combinations are differentiated with respect to the size of the information set (with up to about 120 predictors), their conditional mean and variance parameterization, and several MIDAS weighting schemes. We apply these models for now- and forecasting quarterly annualized real GDP growth and inflation in the GDP deflator with monthly predictors in a large-scale pseudo real time evaluation scheme. Here, we consider a long holdout period starting in the late 1980s. Predictive inference is then based on various point, density and tail forecast losses.

There are several findings to report. First, nonlinear means are relatively more important when trying to improve forecasts. But their out-of-sample performance is also competitive when the focus is on nowcasting. The GP outperforms BART among the nonparametrics and SV is an important model feature irrespective of other specification details. Second, the size of the information set matters a bit more for linear competitors; the nonparametric versions typically perform well already with small data input. Relatedly, unrestricted MIDAS versions are seldom among the best performing specifications, and putting structure on the predictors with specific lag polynomials is beneficial in most cases. Third, the nonparametric models are strongest when the least information is available. For instance, they perform better on average for somewhat longer-horizon predictions, and when the economy is in recession.

The rest of the paper is structured as follows. Section 2 presents the econometric framework. Section 3 contains the empirical application on short-horizon predictions of growth and inflation. Section 4 summarizes the main findings and concludes.

² [Breitung and Roling \(2015\)](#) develop classical small-scale homoskedastic nonparametric MIDAS models, showing that they perform well for predicting inflation using daily data.

2. ECONOMETRIC FRAMEWORK

Let $\{y_t\}_{t=1}^{T_L}$ denote a scalar target variable and $\{\mathbf{x}_t\}_{t=1}^{T_L}$ is an $M \times 1$ -vector comprised of predictors on the lowest of two or more frequencies, observed T_L times. In this paper we consider direct predictive regressions of the form:

$$y_t = f(\mathbf{x}_{t-h}) + \epsilon_t, \quad \epsilon_t \sim \mathcal{N}(0, \sigma_t^2). \quad (1)$$

We will focus on nowcasts or very short-horizon forecasts in our empirical work but note that this framework may also be used for multi-step-ahead predictions. The (potentially unknown and nonlinear) conditional mean function $f : \mathbb{R}^M \rightarrow \mathbb{R}$ will be specified below, and ϵ_t is a zero mean conditionally Gaussian error term with variance σ_t^2 .

The mixed frequency aspects of our work are due to the vector \mathbf{x}_t is constructed. The goal is to model the low frequency variable as a function of high frequency variables. The easiest way to achieve this is to work on a single frequency, i.e., to aggregate all series to the respective lowest frequency (e.g., by considering averages or end-of-period values). But this poses the risk of ignoring potentially useful within-period variation. Let $\{z_t\}_{t=1}^{T_H}$ with $z_t = (z_{1t}, \dots, z_{Kt})'$ denote a K -vector of variables observed T_H times on a higher frequency. Further, $\tilde{z}_{kt} = (z_{kt}, z_{kt-1/m}, z_{kt-2/m}, \dots, z_{kt-(P_H-1)/m})'$ is a $P_H \times 1$ -vector of high frequency lags of the k th predictor. Assuming an evenly spaced frequency mismatch between the target and the predictors yields an integer ratio $m = T_H/T_L$; m thus indicates how often the high frequency variables are observed in terms of one observation of the low frequency variable.³ Moreover, \mathbf{W}_m is a $P_H \times L$ matrix of weights where m refers to a specific MIDAS variant.

In our empirical work, the vector \mathbf{x}_t contains P_L lags of the dependent variable and P_H lags of the K predictors:⁴

$$\mathbf{x}_t = (y_{t-1}, \dots, y_{t-P_L}, \tilde{z}_{1t}' \mathbf{W}_m, \dots, \tilde{z}_{Kt}' \mathbf{W}_m)',$$

³ For instance, when linking a quarterly dependent variable to monthly predictors there are three months per quarter and we have $m = 3$. In this case, $t - 2/3$ and $t - 1/3$ refer to the first and second month by quarter t , respectively. This can easily be relaxed to uneven frequency mismatches and multiple frequencies, which we avoid here to keep the notation simple.

⁴ The vector of predictors \mathbf{x}_t can trivially be augmented to include deterministic terms, lags of other low frequency variables and latent or observed factors.

such that $M = P_L + KL$. The collection of weighting functions is called a dictionary in the related literature (see [Babii et al., 2022](#)), so L is the size of said dictionary. Loosely speaking, the matrix of weights maps the P_H -sized k th predictor vector to a (usually) lower dimension L , thereby reducing the number of parameters that need to be estimated (at least in the common default case). And MIDAS regressions can roughly be classified to be either unrestricted or restricted with various sub-categories. These in essence result from specifics about \mathbf{W}_m and choices about L . We discuss these aspects next.

2.1. Unrestricted and restricted MIDAS

When using U-MIDAS (abbreviated u later) we have $L = P_H$ and $\mathbf{W}_u = \mathbf{I}_{P_H}$ where \mathbf{I}_{P_H} refers to a P_H -dimensional identity matrix. Hence, for each additional high frequency indicator, U-MIDAS results in P_H additional covariates in Eq. (1), leading to a rapid increase in the number of parameters, since $M = P_L + KP_H$. For an overview and a more detailed discussion, see [Foroni et al. \(2015\)](#).

Restricted MIDAS specifications alleviate overparameterization concerns via setting $L < P_H$. Several comparatively parsimonious parameterizations of the respective lag polynomials and thus the weight function are available. In many cases it is convenient to impose specific shapes on the weights and thus emphasize distinct high frequency lags; for instance, to reflect that more recent lags are usually more important than more distant ones. A prominent and often used example with $L = 1$ is the so-called exponential Almon lag, which we abbreviate `xal`. This collapses the matrix \mathbf{W}_{xal} to a $P_H \times 1$ -vector and an implementation with two parameters sets its elements to $(\exp(\theta_1 r) + \exp(\theta_2 r^2)) / (\sum_{r=0}^{P_H-1} \exp(\theta_1 r) + \exp(\theta_2 r^2))$ for $r = 0, \dots, P_H - 1$. Estimating these parameters allows for straightforward data driven high frequency lag selection. It is worth mentioning, however, that this may come with a computational cost, particularly if the number of predictors is huge. A trivial special case arises for $\theta_1 = \theta_2 = 0$ which yields equal weights. This is commonly referred to as a bridge model (abbreviated `br` in what follows), and represents the simplest case that we consider in our empirical work.

While this parsimonious low-dimensional parameterization already typically works well in practice, the more recent literature suggests that $L > 1$ cases offer additional flexibility that may result in improvements of predictive performance. The next scheme we consider is in line with [Mogliani and Simoni \(2021\)](#) and referred to as Almon polynomial of degree

L , abbreviated alm-L. Here, we set the $(l + 1)$ th column of the weighting matrix $\mathbf{W}_{\text{alm-L}}$ to $[0^l, 1^l, 2^l, \dots, (P_H - 1)^l]'$ for $l = 0, \dots, L - 1$, and normalize the sums of the columns to one. Babii *et al.* (2022) discuss further options among the class of orthogonal algebraic polynomials. They suggest to use so-called Legendre polynomials of degree L (labeled leg-L), which are a special case of Jacobi polynomials with various favorable properties.

These considerations yield to our set the restricted and U-MIDAS versions, which is indexed by $\mathbf{m} \in \{\text{br}, \text{xalm}, \text{alm-L}, \text{leg-L}, \text{u}\}$.

2.2. Modeling the conditional mean

Rather than assuming a specific functional form we treat the conditional mean function $f(\mathbf{x}_{t-h})$ as unknown in our most general specifications and estimate it using a GP prior (see Williams and Rasmussen, 2006). That is, we place a prior directly on the functional relationship:

$$f(\mathbf{x}_{t-h}) \sim \mathcal{GP}(0, \mathcal{K}_{\kappa}(\mathbf{x}_{t-h}, \mathbf{x}_{t-h})),$$

where $\mathcal{K}_{\kappa}(\bullet)$ denotes a suitable covariance function (the kernel) which we define below. Stacking over time we obtain $\mathbf{f} = (f(\mathbf{x}_{1-h}), \dots, f(\mathbf{x}_{T_L-h}))'$ and $\mathbf{X} = (\mathbf{x}_{1-h}, \dots, \mathbf{x}_{T_L-h})'$,⁵ and this prior takes the form of a T_L -dimensional multivariate Gaussian distribution:

$$\mathbf{f} \sim \mathcal{N}(\mathbf{0}, \mathcal{K}_{\kappa}(\mathbf{X}, \mathbf{X}')), \quad (2)$$

with the (t, \tilde{t}) th element of $\mathcal{K}_{\kappa}(\mathbf{X}, \mathbf{X}')$ given by $\mathcal{K}_{\kappa}(\mathbf{x}_t, \mathbf{x}_{\tilde{t}})$. In simple terms, the value of the covariance function governs the prior similarity of the functional values between time t and \tilde{t} based on comparing the input vectors \mathbf{x}_t and $\mathbf{x}_{\tilde{t}}$. It is thus common to assume a kernel based on a simple distance measure, and we rely on the squared Euclidean norm to define $d_{t\tilde{t}} = \|\mathbf{x}_t - \mathbf{x}_{\tilde{t}}\|^2$. In particular, we use a squared exponential kernel $\mathcal{K}_{\kappa}(\mathbf{x}_t, \mathbf{x}_{\tilde{t}}) = \varphi \times \exp(-\frac{\varrho}{2}d_{t\tilde{t}})$, where the hyperparameters $\kappa = (\varphi, \varrho)'$ are the unconditional variance φ of the prior, and the inverse length-scale ϱ , which governs the shape of the prior conditional mean functions.⁶

Bayesian inference is based on manipulating a multivariate Gaussian distribution given by Eq. (2), which in stacked notation is $\mathbf{y} \sim \mathcal{N}(\mathbf{0}, \mathcal{K}_{\kappa}(\mathbf{X}, \mathbf{X}') + \mathbf{\Sigma})$, using $\mathbf{\Sigma} = \text{diag}(\sigma_1^2, \dots, \sigma_{T_L}^2)$.

⁵ Our notation here does not rule out the possibility of negative subscripts on early observations. In practice, we truncate our sampling period accordingly by h observations and do not explicitly address initial conditions.

⁶ There are many other possibilities to parameterize the kernel. We have experimented with alternative options but found the squared exponential kernel to perform well consistently.

Computationally, this implies operations with matrices that are at most T_L dimensional. The size of the input space, i.e., the number of predictors M is by and large unimportant with respect to computational performance. This makes GPs particularly attractive for the MIDAS case, because on the one hand we work with the lowest of all available frequencies, which means the least amount of observations. The side effect of increasing the number of predictors (particularly in the case of U-MIDAS), on the other hand, does not affect our framework other than implying a different distance metric in the kernel.

ALTERNATIVES. We argued above that the GP prior is well-suited for the MIDAS framework, due to how the variables are handled and the rather general form of nonlinearities it is able to capture. There are, however, alternative ways of how to estimate the function $f(\mathbf{x}_{t-h})$ and choosing the GP as a specific way is to some extent arbitrary. Among these alternatives are, for instance, regression trees. In our empirical work we consider a Bayesian implementation as a competing specification. In particular, we rely on BART, and assume:

$$f(\mathbf{x}_{t-h}) \approx \sum_{s=1}^S \ell_s(\mathbf{x}_{t-h} | \mathcal{T}_s, \boldsymbol{\mu}_s),$$

where \mathcal{T}_s denotes the tree structure, $\boldsymbol{\mu}_s$ is a vector of terminal node parameters associated with each tree, and we have $s = 1, \dots, S$, regression trees. For these we use the default prior setup and tuning parameters suggested in [Chipman *et al.* \(2010\)](#), which have been shown to work well also in a time series context (see, e.g., [Clark *et al.*, 2023](#)). We set $S = 250$.

Another important variation is the linear version of the MIDAS regression, which we achieve with:

$$f(\mathbf{x}_{t-h}) = \mathbf{x}_{t-h}' \boldsymbol{\beta},$$

where $\boldsymbol{\beta}$ is an $M \times 1$ vector of regression coefficients. This represents the basic framework used in recent related papers that are inspired by the machine learning literature. An example for a classical econometric implementation is [Babii *et al.* \(2022\)](#), while a Bayesian version is developed in [Mogliani and Simoni \(2021\)](#). Methodologically, both of these papers use grouped shrinkage on the regression parameters, where groups are comprised of the L weighted high frequency lags for each of the K predictors. Another noteworthy example is [Kohns and Potjagailo \(2023\)](#), who add a time-varying intercept term and t -distributed errors with stochastic volatility.

Our approach to inference in this case is closely related. We impose global-local shrinkage on the regression parameters β with a horseshoe prior (HS, [Carvalho *et al.*, 2010](#)). Below we refer to this specification as Bayesian linear regression (BLR).

2.3. Other specification details

ERROR VARIANCE. For the case of homoskedastic errors (labeled `hom`), we assume $\sigma_t^2 = \sigma^2$ and $\sigma^2 \sim \mathcal{G}^{-1}(a_0, b_0)$. To introduce SVs, similar to [Pettenuzzo *et al.* \(2016\)](#) but without predictors in the state equation, let $\varsigma_t = \log(\sigma_t^2)$ and assume:

$$\varsigma_t = \mu_\varsigma + \phi_\varsigma(\varsigma_{t-1} - \mu_\varsigma) + \sigma_\varsigma \zeta_t, \quad \zeta_t \sim \mathcal{N}(0, 1). \quad (3)$$

We rely on the prior setup of [Kastner and Frühwirth-Schnatter \(2014\)](#), and assume a Gaussian prior for the unconditional mean $\mu_\varsigma \sim \mathcal{N}(0, 10)$, a transformed Beta prior for the autoregressive parameter $(\phi_\varsigma + 1)/2 \sim \mathcal{B}(5, 1.5)$, and a Gamma prior on the state innovation variances $\sigma_\varsigma^2 \sim \mathcal{G}(1/2, 1/2)$. The prior on the initial state is $\varsigma_h \sim \mathcal{N}(\mu_\varsigma, \sigma_\varsigma^2/(1 - \phi_\varsigma^2))$.

TUNING PARAMETERS. The final sets of parameters for which we need to choose priors are those that govern `xalm`, and the hyperparameters of the GP prior. For the former, we use weakly informative independent Gaussian priors. For the latter, we use a mildly informative Gamma prior on the unconditional variance of the prior φ , and a somewhat tighter Gamma prior on the inverse length-scale ϱ . Prior information on ϱ is imposed to reduce the risk of overfitting, and to gently push the GP prior towards a linear relationship.

2.4. Posterior and predictive inference

Let $\boldsymbol{\vartheta}$ denote a vector of all parameters that need to be estimated for each model variant and $\mathcal{D}_{1:t}$ refers to the information set that is available up to time t . In its general form, the predictive distribution is given by $p(y_{t+h}|\mathbf{x}_t, \mathcal{D}_{1:t}) = \int p(y_{t+h}|\mathbf{x}_t, \boldsymbol{\vartheta})p(\boldsymbol{\vartheta}|\mathcal{D}_{1:t})d\boldsymbol{\vartheta}$. This distribution can be explored using Monte Carlo techniques, which amounts to sampling from the conditional distribution $y_{t+h} \sim \mathcal{N}(f(\mathbf{x}_t), \sigma_{t+h}^2)$ in each sweep of our algorithm.

To sample from this conditional predictive distribution we need to produce draws from the respective conditional distribution of $f(\mathbf{x}_t)$ and that of σ_{t+h}^2 . The joint posterior distribution is not of a well-known form, and we therefore use several Metropolis-Hastings steps within a Gibbs sampling algorithm. Our algorithm cycles through the following steps:

1. **Updating the conditional mean.** Given the conditional variances Σ and the predictors \mathbf{X} , we can update the conditional mean for our three different alternatives:

(a) **GP.** In this case, we can sample $\mathbf{f} \sim \mathcal{N}(\bar{\mathbf{f}}, \bar{\mathbf{V}})$ from a multivariate Gaussian:

$$\begin{aligned}\bar{\mathbf{f}} &= \mathcal{K}_{\kappa}(\mathbf{X}, \mathbf{X}')(\mathcal{K}_{\kappa}(\mathbf{X}, \mathbf{X}') + \Sigma)^{-1} \mathbf{y} \\ \bar{\mathbf{V}} &= \mathcal{K}_{\kappa}(\mathbf{X}, \mathbf{X}') - \mathcal{K}_{\kappa}(\mathbf{X}, \mathbf{X}')(\mathcal{K}_{\kappa}(\mathbf{X}, \mathbf{X}') + \Sigma)^{-1} \mathcal{K}_{\kappa}(\mathbf{X}, \mathbf{X}'),\end{aligned}$$

and update $f(x_t)$ analogously.

(b) **BART.** For this option, we update \mathbf{f} and $f(x_t)$ by following the sampling procedure proposed in [Chipman *et al.* \(2010\)](#). This involves two main steps. First, we update the tree structures using a Metropolis-Hastings step marginal of the terminal node parameters. Second, we update the terminal node parameters from a Normal distribution conditional on the tree structure.

(c) **BLR.** We can sample β from its conditional posterior, which is multivariate Normal distribution. It is worth noting that we use the fast-sampling algorithm of [Bhattacharya *et al.* \(2016\)](#) for BLR when $T_L < M$, because estimation turns out to be infeasible in a reasonable amount of time with a default setup (e.g., for U-MIDAS with larger information sets). The posterior mean and posterior variance of this distribution are of standard form and can be found in any Bayesian textbook (e.g., [Koop, 2003](#)). Then, we have $f(x_t) = x_t' \beta$.

2. **Updating the conditional variances.** Given a draw for the conditional mean \mathbf{f} , the error variance or its prediction can be sampled from:

- (a) a well-known inverse Gamma posterior distribution in the case of homoskedastic errors;
- (b) through sampling the log-volatilities $\varsigma_1, \dots, \varsigma_t, \dots, \varsigma_{t+h}$ with filtering algorithms for state space models based on state Eq. (3), see e.g., [Kastner and Frühwirth-Schnatter \(2014\)](#).

3. **Updating tuning/hyperparameters.** The prior variances from the global-local prior setup for the linear regression coefficients can be updated by sampling from inverse Gamma distributions using an auxiliary representation of the HS. All remaining parameters like the hyperparameters of the GP prior or the MIDAS-parameters for `xalim` are drawn using Metropolis-Hastings updates with a random walk proposal.

In our empirical work, we iterate the sampling algorithm for 12,000 times; then we discard the initial 3,000 as burn-in and use each third of the remaining draws for inference. This yields a set of 3,000 draws to be used for computing any object or moment of interest.

3. NOWCASTING AND FORECASTING US OUTPUT AND INFLATION

3.1. Data, competing models and predictive losses

The quarterly target series are sourced from FRED-QD and the monthly predictors are from the FRED-MD database (see [McCracken and Ng, 2016; 2020](#)). Our target variables are real GDP growth (GDPG1) and inflation in the GDP deflator (GDPCTPI). Both are used in the form of annualized growth rates.

Our predictors are defined based on differently sized information sets: a *small* ($s, K = 12$), *medium* ($m, K = 23$) and *Big Data* ($b, K = 116$) one. These sets are constructed such that the respective larger one nests the smaller ones. A detailed description of which predictors are used in each of them is provided in the Appendix. All these predictor variables are processed using the suggested transformation codes to achieve approximate stationarity. We use $P_L = 4$ lags of the target variable as is common with quarterly data; and, reflecting the month/quarter frequency mismatch, we set $P_H = 12$ based on $P_H = mP_L$ for consistency. In line with [Mogliani and Simoni \(2021\)](#) and [Babii et al. \(2022\)](#), we choose $L = 3$ when applicable.

In the out-of-sample evaluation scheme, we rely on final vintage data but truncate each one of the training samples according to the release calendar as we simulate moving forward in time. Our full sampling period runs from 1963Q1 to 2023Q2, and our initial estimation (training) samples end in 1986Q4, such that the first targeted quarter in our holdout sample is 1987Q1. We note that the generic notation x_{t-h} thus does not mean in our pseudo out-of-sample context that, e.g., $h = 0$ in Eq. (1) defines a contemporaneous regression, but rather that we leverage all information available at time t to produce the nowcast.⁷

Our predictions for horizon h are updated at the end of each month during the quarter:

$$h \in \left\{ \underbrace{0, \frac{1}{3}, \frac{2}{3}}_{\text{nowcast}}, \underbrace{1, \frac{4}{3}, \frac{5}{3}}_{\text{forecast}} \right\}.$$

⁷ For instance, to nowcast GDP in the final month of 2023Q1, we would only have access to monthly industrial production data ranging until 2023M2.

Table 1: Design of the forecast exercise and competing models.

MIDAS	Mean	Variance
Unrestricted, $L = P_H$ (u)	Linear (BLR): $f(\mathbf{x}_{t-h}) = \mathbf{x}'_{t-h}\boldsymbol{\beta}$	$\sigma_t^2 = \sigma^2$ (hom)
$L = 1$ (br, xalm)	GP: $f(\mathbf{x}_{t-h}) \sim \mathcal{GP}(0, \mathcal{K}_{\kappa}(\mathbf{x}_{t-h}, \mathbf{x}_{t-h}))$	σ_t^2 (sv)
$L = 3$ (alm-3, leg-3)	BART: $f(\mathbf{x}_{t-h}) \approx \sum_{s=1}^S \ell_s(\mathbf{x}_{t-h} \mathcal{T}_s, \boldsymbol{\mu}_s)$	

Notes: All specifications target real GDP growth (GDPC1) or the GDP deflator (GDPCTPI) with small (s, $K = 12$), medium (m, $K = 23$), big data (b, $K = 116$) information sets for nowcasts $h \in \{0, 1/3, 2/3\}$ and forecasts $h \in \{1, 4/3, 5/3\}$. Number of predictors: $M = P_L + KL$, which results in approximately 1.4k predictors in our most flexible specification. In combination with the length of our holdout sample, we run about 160k models in our out-of-sample simulation.

Besides differently sized information sets, our set of competing models is defined as follows. We vary the respective approach to estimating the conditional means $f(\bullet)$ by using linear (BLR), GP and BART versions. In addition, we consider homoskedastic (hom) and heteroskedastic (sv) implementations. The final variation is due to how we construct the design matrices with respect to distinct MIDAS-types. Here, we use both U-MIDAS and the restricted approaches we discussed in Section 2.1. As a simplistic benchmark, we also estimate univariate $AR(P_L)$ models which are updated each quarter.

An overview is provided in Table 1. When we explicitly refer to a model in the text, we structure their IDs as mean-variance-midas-size.

Loss Functions. We evaluate our forecasts using several distinct loss functions that measure different aspects of predictive accuracy. Specifically, we use the quantile score (QS) and the (quantile-weighted) continuous ranked probability score (CRPS), see [Giacomini and Komunjer \(2005\)](#), [Gneiting and Raftery \(2007\)](#).

The QS for quantile $\tau \in (0, 1)$ of the forecast of target variable y_t is defined as $QS_{\tau,t} = 2(y_t - \hat{y}_{\tau,t})(\tau - \mathbb{I}\{y_t \leq \hat{y}_{\tau,t}\})$, where $\hat{y}_{\tau,t}$ indicates the τ th quantile of the predictive distribution. The indicator function $\mathbb{I}\{y_t \leq \hat{y}_{\tau,t}\}$ has a value of 1 if the realized value is at or below the quantile forecast, and 0 otherwise. Note that $QS_{0.5,t}$ is the absolute error (which we use in the form of the mean absolute error, MAE, as our point forecast loss).

Using the QS, we can then define the quantile-weighted CRPS following [Gneiting and Ranjan \(2011\)](#):

$$CRPS-V_t = \int_0^1 w_{V,\tau} QS_{\tau,t} d\tau, \quad \text{for: } V \in \{L, R\},$$

where $w_{V,\tau}$ indicate weights that put emphasis on different parts of the distribution. The default CRPS results when we use equal weights, but we also consider different weighting

schemes that target the left tail $w_{L,\tau} = (1 - \tau)^2$ and the right tail $w_{R,\tau} = \tau^2$. We approximate the integral above with a sum based on a grid of quantiles, $\tau \in \{0.05, 0.06, \dots, 0.94, 0.95\}$.

3.2. A bird's-eye view of useful model features

The set of competing models is large, so we slice our empirical results along several dimensions to provide a concise overview. Our first set of results in this regard is constructed as follows. We choose the CRPS averaged for various subsamples over the holdout as our metric of choice for measuring overall forecast performance by target variable.⁸ The logarithms of these losses across specifications are then regressed on dummies comprised of the categories determined by the underlying means, variances, sizes of the information set and MIDAS-type. As baseline category, we choose the linear homoskedastic bridge model estimated with the small information set (i.e., BLR-hom-br-s). The parameters are estimated with OLS and multiplied by 100. These are the numbers shown in Figure 1, which can be interpreted as percentage gains/losses due the extensions indicated in the rows of each individual panel relative to the losses of the benchmark. The columns refer to the nowcast/forecast horizon h .⁹

A striking finding considering the color patterns in different shades of blue/red (indicating that the respective feature reduces/increases losses relative to the reference category) is, ignoring magnitudes for the moment, that they are rather stable across subsample splits and target variables. But there are also some exceptions to this statement.

Addressing choices about the conditional mean first, we find that the nonparametric models pay off particularly as h becomes large. By contrast, for the nowcasts, we find that GP and BART are often performing worse than when assuming linearity a priori (sometimes even significantly so). A striking finding is also that the nonparametric models perform comparatively poorly for inflation during recessions. It is worth noting, however, that this overview abstracts from interactions of model features. So even when on average losses are larger when moving from BLR to GP or BART, keeping everything else fixed, this is not necessarily the case for distinct model specifications. Indeed, we zoom into model-specific performance below and find that several versions of the GP implementation are in fact the overall best performing models.

⁸ Subsamples are: Full denotes the whole (holdout) sample from 1987Q1 until 2023Q2, which is split at 2019Q4 into Pre Covid and Post Covid. We further differentiate Recession versus Expansion by considering all dates qualified as falling into a recessionary period by NBER as the former, and the rest of the sample as the latter.

⁹ When using the MAE instead as explained loss we obtain qualitatively very similar patterns. These results are available upon request.

Full		GDPC1						GDPC1						GDPC1						GDPC1						GDPC1					
		GP	7.5°	-1.0	2.8°	-5.4°	-9.6°	-7.5°	GP	7.5°	-1.0	2.8°	-5.4°	-9.6°	-7.5°	GP	4.0°	2.3°	-1.0	-1.9°	-4.6°	-6.4°	GP	3.7°	6.2°	4.6°	0.1	-0.8	-3.5°		
	BART	12.2°	3.3°	6.6°	-2.6°	-5.4°	-2.3°	BART	10.6°	6.2°	4.1°	-1.9	-7.4°	-5.0°	BART	5.7°	4.1°	0.9	-1.2	-2.1°	-3.7°	BART	11.7°	10.2°	5.5°	0.4	-3.7	-3.5°			
	xalm	-22.8°	-14.5°	-13.1°	-1	0.1	-0.7	-0.5	xalm	-9.3°	-8.3°	-5.7°	-2.8	0.7	-3.9°	xalm	-11.2°	-13.6°	-3.9°	-1.8°	-1.4	-0.9	xalm	-3.6°	-5.2°	-1.8	-1.1	1.0	-1.4		
	alm-3	-9.3°	-5.4°	-0.8	1.0	0.4	0.1	-0.6	0.5	2.7	1.8	3.2°	2.2	alm-3	0.9	-0.8	1.8	1.3	2.1°	0.3	alm-3	1.9	3.6	4.0°	4.0°	3.5	1.9				
	leg-3	-15.5°	-7.5°	-4.4°	1.2	-0.6	0.7	4.0°	7.2°	7.7°	3.4°	6.8°	2.8	leg-3	-6.7°	-9.2°	-4.0°	-1.8°	-1.3	-1.0	leg-3	6.4°	7.5°	8.2°	3.9°	7.6°	5.0°				
	u	-12.5°	-7.8°	-9.1°	-1.0	0.7	2.1°	2.7	5.8°	8.4°	2.4	4.1°	0.1	u	-2.9°	-5.2°	0.4	0.7	2.1°	1.2	u	8.9°	11.4°	11.1°	5.7°	6.6°	2.8				
	m	-0.6	0.3	0.3	0.0	0.0	0.1	-1.3	-1.3	0.1	0.0	0.9	1.0	m	2.3°	1.4	0.8	0.9	1.0	0.8	m	0.3	-1.2	1.2	1.3	1.7	1.8				
	b	0.5	1.7	2.4	0.9	1.3	1.6°	1.4	-1.3	-0.7	1.7	3.5°	4.7°	b	7.0°	7.1°	3.9°	2.2°	2.4°	1.9°	b	5.3°	4.1°	5.3°	8.0°	8.9°	9.5°				
	sv	-4.5°	-2.4°	-4.4°	-1.8°	-2.5°	-1.4°	-2.7°	-3.2°	-2.7°	-5.9°	-8.1°	-8.4°	sv	-0.8	-0.9	-1.7°	-4.1°	-3.1°	-2.7°	sv	-3.0°	-4.4°	-3.7°	-7.0°	-8.5°	-8.0°				
h	0	1/3	2/3	1	4/3	5/3	h	0	1/3	2/3	1	4/3	5/3	h	0	1/3	2/3	1	4/3	5/3	h	0	1/3	2/3	1	4/3	5/3				
Recession		GDPC1						GDPC1						GDPC1						GDPC1						GDPC1					
		GP	4.7°	0.6	5.8°	5.9°	3.7°	-3.1°	GP	4.7°	0.6	5.8°	5.9°	3.7°	-3.1°	GP	8.0°	-1.2	2.3	-7.4°	-12.2°	-8.3°	GP	6.4°	6.3°	2.6	-7.4°	-10.7°	-10.2°		
	BART	12.1°	2.0	4.4°	3.7°	7.5°	-1.9°	BART	27.5°	25.1°	19.4°	28.0°	26.9°	25.8°	BART	12.4°	3.6°	7.0°	-3.7°	-7.9°	-2.4°	BART	8.1°	4.0°	2.4	-5.1°	-10.9°	-7.9°			
	xalm	-15.5°	-21.7°	-17.5°	-8.8°	-5.1°	-7.9°	xalm	-1.5	-2.2	-0.8	0.2	3.1	4.0	xalm	-23.6°	-13.4°	-12.4°	1.7	0.2	1.0	xalm	-10.3°	-9.0°	-6.3°	-3.1°	0.4	-4.6°			
	alm-3	0.8	-2.3	1.5	0.2	1.2	-0.2	alm-3	-2.9	0.9	4.1	-4.5	-0.2	-5.3	alm-3	-10.6°	-5.8°	-1.1	1.1	0.3	0.1	alm-3	-0.3	0.4	2.6	2.6	3.6°	2.7			
	leg-3	-11.7°	-13.0°	-16.8°	-9.4°	-5.3°	-7.8°	leg-3	9.1°	6.8	2.7	-1.8	0.0	-2.7	leg-3	-15.9°	-6.6°	-2.5	3.1°	0.4	2.4°	leg-3	3.4	7.3°	8.3°	3.9°	7.5°	3.7°			
	u	3.5	-2.1	-4.2°	-3.9°	-3.9°	-2.6°	u	-1.3	8.0°	0.5	-6.6	0.1	5.2	u	-14.6°	-8.7°	-9.8°	-0.4	1.7	3.1°	u	3.2	5.6°	9.4°	3.4°	4.6°	-0.4			
	m	1.5	3.5	2.9°	3.3°	1.7	-1.4	m	0.6	-7.2°	5.1°	0.4	-0.6	4.3	m	-0.9	-0.2	-0.1	-0.6	-0.4	0.4	m	-1.5	-0.6	-0.5	0.0	1.0	0.7			
	b	11.9°	12.1°	8.0°	6.1°	2.3°	-0.7	b	-8.6°	-10.8°	3.0	1.7	4.1	4.7°	b	-1.1	0.2	1.6	0.0	1.1	2.0°	b	2.7	-0.2	-1.1	1.8	3.5°	4.5°			
	sv	2.0	1.9	5.7°	-1.3	-1.0	2.5°	sv	-1.9	0.5	-0.9	-7.0°	-5.9°	-3.8°	sv	-5.3°	-3.0°	-5.9°	-1.9°	-2.8°	-2.1°	sv	-2.8°	-3.6°	-2.9°	-5.7°	-8.3°	-8.8°			
h	0	1/3	2/3	1	4/3	5/3	h	0	1/3	2/3	1	4/3	5/3	h	0	1/3	2/3	1	4/3	5/3	h	0	1/3	2/3	1	4/3	5/3				
Post Covid		GDPC1						GDPC1						GDPC1						GDPC1						GDPC1					
		GP	17.5°	-5.6	14.3°	-11.2°	-18.6°	-9.8°	GP	14.2°	11.5°	-0.1	-17.5°	-25.6°	-18.5°	GP	7.5°	-5.2°	0.8	-6.3°	-15.1°	-8.0°	GP	7.5°	-5.2°	0.8	-6.3°	-15.1°	-8.0°		
	BART	27.2°	3.3	21.4°	-4.7°	-11.1°	0.1	BART	7.5°	-5.2°	0.8	-6.3°	-15.1°	-8.0°	BART	7.5°	-5.2°	0.8	-6.3°	-15.1°	-8.0°	BART	7.5°	-5.2°	0.8	-6.3°	-15.1°	-8.0°			
	xalm	-43.1°	-15.9°	-32.4°	3.4	0.9	0.3	xalm	-26.6°	-17.1°	-17.4°	-6.1°	0.0	-9.7°	xalm	-26.6°	-17.1°	-17.4°	-6.1°	0.0	-9.7°	xalm	-26.6°	-17.1°	-17.4°	-6.1°	0.0	-9.7°			
	alm-3	-26.5°	-13.6°	-4.9	0.4	-2.4	-0.4	alm-3	-7.2°	-7.7°	-0.1	-2.8	2.6	3.3	alm-3	-7.2°	-7.7°	-0.1	-2.8	2.6	3.3	alm-3	-7.2°	-7.7°	-0.1	-2.8	2.6	3.3			
	leg-3	-29.7°	-4.5	-4.9	6.2°	1.1	3.9°	leg-3	-3.3	6.1	6.4	2.3	4.0	-2.4	leg-3	-3.3	6.1	6.4	2.3	4.0	-2.4	leg-3	-3.3	6.1	6.4	2.3	4.0	-2.4			
	u	-27.9°	-12.6°	-30.3°	-4.1	-1.5	4.0°	u	-15.8°	-9.8°	1.7	-5.5	-2.7	-6.6°	u	-15.8°	-9.8°	1.7	-5.5	-2.7	-6.6°	u	-15.8°	-9.8°	1.7	-5.5	-2.7	-6.6°			
	m	-5.9	-1.5	-0.6	-1.4	-1.7	-1.4	m	-5.6°	-1.7	-3.2	-3.2	-1.5	-1.2	m	-5.6°	-1.7	-3.2	-3.2	-1.5	-1.2	m	-5.6°	-1.7	-3.2	-3.2	-1.5	-1.2			
	b	-11.9°	-7.5°	0.5	-1.1	-0.6	0.9	b	-10.1°	-16.8°	-20.1°	-14.7°	-10.3°	-7.9°	b	-10.1°	-16.8°	-20.1°	-14.7°	-10.3°	-7.9°	b	-10.1°	-16.8°	-20.1°	-14.7°	-10.3°	-7.9°			
	sv	-10.9°	-4.8°	-9.1°	2.6	-1.0	1.2	sv	-1.9	0.3	0.3	-2.8	-6.8°	-8.9°	sv	-1.9	0.3	0.3	-2.8	-6.8°	-8.9°	sv	-1.9	0.3	0.3	-2.8	-6.8°	-8.9°			
h	0	1/3	2/3	1	4/3	5/3	h	0	1/3	2/3	1	4/3	5/3	h	0	1/3	2/3	1	4/3	5/3	h	0	1/3	2/3	1	4/3	5/3				

The largest relative gains, on the other hand, are available when adjusting lag polynomials. The two-parameter specification `xa1m` seems to succeed in striking a balance between flexibility and simplicity. The corresponding accuracy premium appears consistently across horizons and target variables, although the magnitudes differ somewhat. Taking the full sample as an example, we find that for the final nowcast per quarter ($h = 0$, when most information is already available), moving from the simplistic bridge model to `xa1m`-MIDAS reduces losses by about 23 percent, holding all other model features fixed. We also note that U-MIDAS is competitive in many cases, but its performance is not as consistent across horizons and subsamples as some of the restricted versions.

significantly hurts predictive accuracy by a few percent. For the post Covid period, however, having a larger information set improves performance by up to 10 and 20 percent depending on the target and horizon.

3.3. Model-specific results

The discussion in the previous subsection relied on *ceteris paribus* interpretations and thus abstracted from interaction effects of model components. To drill deeper into model-specific predictive accuracy, we select a subset of models that perform best on average. We benchmark these results relative to an $AR(P_L)$ -model which is a useful baseline for short-horizon forecasts of output growth and inflation. It also reflects the case where no within-quarter information is used. Relative losses are shown as ratios in Table 2, and the models are selected based on the sum of the CRPS across all horizons being minimal. We then display only the best model grouped by specification of the means, for each target variable. Below we mostly focus on discussing the CRPS, since differences between point and density forecasts are often muted.

Overall we find that most of our considered specifications improve upon the $AR(P_L)$ -benchmark, and in many cases they do so significantly. Unsurprisingly the gains are heterogeneous across subsamples, specifications and nowcast/forecast horizons. For output growth, and to a slightly lesser extent also inflation, relative improvements are biggest for nowcasts with the most high frequency information being already available ($h = 0$), and less pronounced for the forecast furthest into the future ($h = 5/3$). This finding is also documented visually in Figure 3 which contains additional model variations. Note that the x-axis which shows horizons is reversed here, i.e., it shows the timeline of relative predictive losses as more information becomes available and forecasts turn into nowcasts. Having access to more current high frequency predictors widens spreads to the benchmark scores. Deviations from this general pattern are present when predicting inflation during recessions.

Many of our findings from the bird’s-eye view translate to the selection of models. We start with a discussion about which models end up in this table based on our selection procedure. First, the MIDAS-type $xa1m$ performs well across all conditional mean specifications, and only in the case of BART we find a different implementation being included in this set of models. Interestingly, and different to BLR and GP, BART seems to be able to better extract information without introducing prior weighting via lag polynomials, though it must be said that this spe-

(a) MAE

		GDPC1						GDPCTPI					
Full	GP-sv-xalm-s	0.80°	0.80°	0.94	0.93°	0.95	0.98	0.92°	0.93°	0.93°	0.93	0.94	0.98
	GP-sv-xalm-b	0.80°	0.84	0.92	0.96	0.98	0.98	0.89°	0.85°	0.85°	0.94	0.98	0.99
	BLR-sv-xalm-m	0.70°	0.86	0.81	1.04	1.07	1.02	0.86°	0.85°	0.89°	0.98	1.05	1.00
	BLR-sv-xalm-b	0.66°	0.84	0.84	1.00	1.01	1.02	0.84°	0.78°	0.90°	0.97	1.04	1.01
	BART-sv-xalm-m	0.85°	0.85°	0.98	0.97	1.03	1.03	0.96	0.90°	0.97	1.01	1.01	1.02
	BART-hom-u-m	0.84°	0.86°	0.94	0.98	1.01	1.02	1.00	1.01	1.01	1.06	1.06	1.05
Pre Covid	GP-sv-xalm-s	0.80°	0.83°	0.96	0.93	0.98	1.01	0.87°	0.85°	0.88°	0.87°	0.90°	0.93
	GP-sv-xalm-b	0.83°	0.89	0.99	0.96	1.02	1.02	0.93	0.85°	0.92	0.97	1.02	1.01
	BLR-sv-xalm-m	0.79°	0.84°	0.95	0.98	1.02	1.04	0.88°	0.82°	0.90°	0.93	0.94	0.96
	BLR-sv-xalm-b	0.78°	0.84°	0.99	0.98	1.02	1.07	0.87°	0.80°	0.93	0.96	0.99	1.01
	BART-sv-xalm-m	0.85°	0.85°	1.01	0.97	1.06	1.08	0.96	0.88°	0.99	1.00	0.99	1.02
	BART-hom-u-m	0.87°	0.90	1.01	1.00	1.02	1.02	1.01	1.00	0.99	1.03	1.03	1.02
Recession	GP-sv-xalm-s	0.48°	0.52°	0.71°	0.73°	0.82°	0.85°	1.09	0.94	0.91	0.89	0.93	0.94
	GP-sv-xalm-b	0.55°	0.65°	0.82	0.84°	0.90°	0.88°	1.09	1.10	1.00	1.10	1.11	1.04
	BLR-sv-xalm-m	0.57°	0.62	0.76	0.79°	0.79°	0.85°	1.00	0.77	0.89	0.76	0.68°	0.72°
	BLR-sv-xalm-b	0.52°	0.69	0.84	0.86°	0.88°	1.01	0.84	0.66	0.93	0.69	0.60	0.59
	BART-sv-xalm-m	0.58°	0.62°	0.78	0.78°	1.03	0.90°	1.28	1.06	1.14	1.18	1.09	1.00
	BART-hom-u-m	0.68°	0.74°	0.84°	0.87°	0.94	0.95	1.08	1.02	0.96	0.97	0.96	1.00
		0	1/3	2/3	1	4/3	5/3	0	1/3	2/3	1	4/3	5/3

h

(b) CRPS

		GDPC1						GDPCTPI					
Full	GP-sv-xalm-s	0.74°	0.73°	0.85°	0.92°	0.94°	0.95°	0.87°	0.88°	0.89°	0.89°	0.89°	0.92°
	GP-sv-xalm-b	0.73°	0.76°	0.84°	0.93°	0.94°	0.96°	0.85°	0.83°	0.83°	0.90°	0.91°	0.93
	BLR-sv-xalm-m	0.63°	0.79°	0.73°	1.00	1.05	1.00	0.82°	0.82°	0.87°	0.92	0.97	0.92°
	BLR-sv-xalm-b	0.59°	0.77°	0.74	0.96	0.99	1.00	0.82°	0.78°	0.87°	0.93	0.98	0.95
	BART-sv-xalm-m	0.80°	0.80°	0.92	0.97	1.00	1.01	0.94	0.90°	0.95	0.97	0.97	0.99
	BART-hom-u-m	0.80°	0.81°	0.88°	0.93°	0.96	0.99	0.98	1.00	1.00	1.01	1.02	1.01
Pre Covid	GP-sv-xalm-s	0.73°	0.74°	0.87°	0.88°	0.92°	0.95°	0.83°	0.82°	0.86°	0.84°	0.86°	0.88°
	GP-sv-xalm-b	0.74°	0.80°	0.91°	0.89°	0.93°	0.96	0.89°	0.85°	0.91°	0.93	0.95	0.96
	BLR-sv-xalm-m	0.71°	0.74°	0.87°	0.91°	0.96	0.99	0.85°	0.79°	0.88°	0.86°	0.87°	0.89°
	BLR-sv-xalm-b	0.70°	0.75°	0.89°	0.90°	0.94°	1.01	0.86°	0.80°	0.91°	0.92	0.94	0.95
	BART-sv-xalm-m	0.79°	0.78°	0.94	0.93°	0.98	1.01	0.97	0.91°	0.98	0.97	0.96	0.99
	BART-hom-u-m	0.81°	0.83°	0.92°	0.92°	0.96	0.97	1.00	0.99	0.99	0.96	0.96	0.96
Recession	GP-sv-xalm-s	0.50°	0.51°	0.65°	0.75°	0.85°	0.89°	1.04	0.93	0.90	0.87	0.88	0.87
	GP-sv-xalm-b	0.57°	0.64°	0.77°	0.86°	0.91°	0.90°	1.03	1.04	0.98	1.02	1.00	0.92
	BLR-sv-xalm-m	0.54°	0.59°	0.73°	0.81°	0.84°	0.92°	1.05	0.77	0.92	0.75	0.70°	0.71°
	BLR-sv-xalm-b	0.52°	0.65°	0.80	0.89°	0.90	1.03	0.90	0.71	0.90	0.74	0.66	0.65
	BART-sv-xalm-m	0.58°	0.61°	0.74°	0.79°	1.03	0.89°	1.29	1.08	1.15	1.19	1.09	1.00
	BART-hom-u-m	0.69°	0.75°	0.83°	0.90°	0.96	0.97	1.05	0.99	0.93	0.90	0.90	0.95
		0	1/3	2/3	1	4/3	5/3	0	1/3	2/3	1	4/3	5/3

h

Fig. 2: Predictive losses for selected specifications relative to the benchmark $AR(P_L)$ -model. *Notes:* Levels of statistical significance $\{5, 1, 0.1\}\%$ for a DM-test of equal predictive accuracy are indicated with $\{', ^\circ, ^\ast\}$. Best-performing specification by horizon in bold.

cification is always beaten by another, more accurate one. Second, adding heteroskedasticity (which we do with sv) definitely pays off. The only exception, again, is BART. This corroborates the findings of [Clark et al. \(2023\)](#), who provide a discussion and some empirical evidence how the regression trees can capture specific forms of heteroskedasticity even when the error terms are homoskedastic.

When turning to the size of the information set, it is worth mentioning that for the GP and BLR cases, we have exactly the same model specification being selected: sv-xalm. Interestingly, for the GP it appears that s is already sufficient to attain good relative predictive losses, and the b-sized version rarely improves upon the small input dataset. By contrast, for BLR, assuming linearity a priori appears to be restrictive, but more information appears to help with this lim-

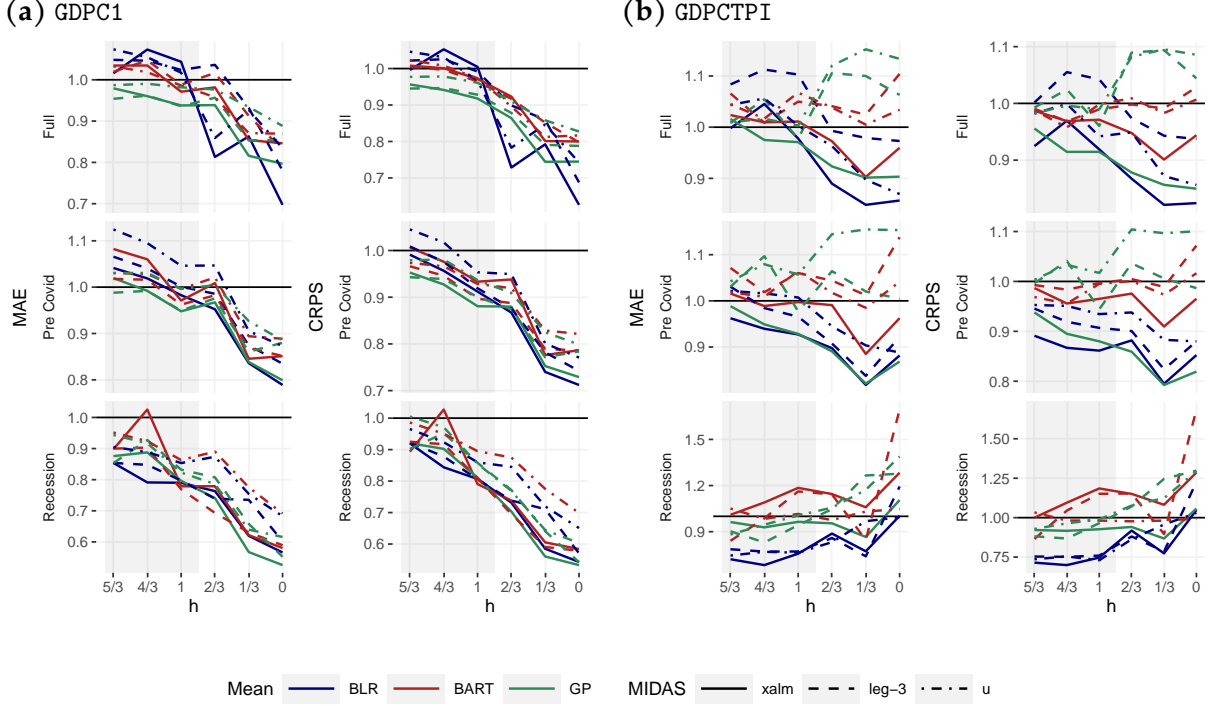


Fig. 3: Predictive losses relative to $AR(P_L)$ -hom (solid black line) by horizon, averaged over the indicated subsample. The grey shade marks the forecasts, no shading indicates nowcasts.

itation. Another interpretation of this pattern is that the nonparametric features offset omitted variables partly, and the bigger the information set becomes, the less there is need for modeling nonlinearities explicitly.

Another related important observation is that BLR is ranked first (indicated by the bold numbers) in many cases for the nowcasts, especially for output. For forecasts, the GP is often better. We conjecture that this is due to the notion that as more information becomes available, the nonlinearities become less emphasized and there is less need for the flexibility in conditional means that our proposed specifications provide. It is worth noting, however, that margins between GP and BLR are often very small (improvements from breaking the linearity assumption with GP, however, reach up to 10 percent depending on subsample splits and the horizon), while BART is slightly worse on average.

We turn to discussing the sample splits in more detail next. Improvements upon the benchmark are sizable during recessions for output growth, that is, arguably those periods when good nowcasts are needed most. Indeed, using GPs approximately halves the respective scores for $h = 0$ and are the overall best performing specification. As the horizon increases, the gains become smaller but they are still 25 percent lower than the $AR(P_L)$ for the one-step ahead

forecast. A different picture emerges for inflation; BART performs worse and also the GPs are dominated by the BLR for most horizons we consider. This points towards instability of forecast performance over the business cycle. When comparing the full sample to the pre-Covid period, we find that the nonparametric models are roughly stable in performance across them, with a noteworthy good performance for forecasts. Interestingly, however, the nonparametric models do a bad job capturing the initial downturn during the pandemic lockdowns, which are captured much more adequately with BLR although the scores are not statistically significantly different from each other.

3.4. Tail forecasting performance

Our previous discussions indicated that models that break the assumption of linearity tend to perform particularly well during nonstandard economic periods such as recessions or when little information is available. To investigate this facet of predictive accuracy in more detail, we now turn to evaluating tail forecast performance by means of the quantile-weighted CRPS. Specifically, we consider CRPS-L and CRPS-R which put emphasis on downside and upside risk respectively. We use the same procedure to select the on average best performing models as before, but now select those where the CRPS for both tails is minimal across horizons. The results for selected subsamples are shown in Table 4.

In general, the vast majority of our model specifications again improve upon now- and forecasts of the $AR(P_L)$ -benchmark (this is especially true for nowcasts and the pre-Covid period), a lot of them by significant margins. The patterns we observe here are rather similar to those we discussed previously in the context of overall point and density forecast accuracy.

Considering left tail forecasts first in the upper panels of Figure 4, several patterns emerge. First, similar to results described above, `sv-xalm` seems to be a powerful combination of model features which almost always make up the best-performing model by each respective horizon. Second, BLR performs relatively well compared to other model specifications when the focus is on nowcasts, however, this only true when BLR can draw from bigger information sets (`m` or `b`). Further into the future, GP specifications gain forecasting performance relative to BLR and are dominant compared to other modeling methods of the conditional mean, with the exception of during recession periods. This is true for both GDP growth and inflation. Interestingly, GP often

(a) CRPS-L

		GDPC1						GDPCTPI					
		0	1/3	2/3	1	4/3	5/3	0	1/3	2/3	1	4/3	5/3
Full	GP-sv-xalm-s	0.77*	0.76°	0.88'	0.93*	0.96*	0.97	0.90°	0.89°	0.92'	0.93	0.93	0.95
	GP-sv-xalm-b	0.75*	0.79°	0.86'	0.95'	0.96	0.98	0.87°	0.86°	0.88*	0.92	0.95	0.96
	BLR-sv-xalm-m	0.62°	0.73*	0.74	0.99	1.03	1.01	0.85°	0.82*	0.90'	0.96	1.00	0.97
	BLR-sv-xalm-b	0.58°	0.73*	0.75'	0.97	0.99	1.01	0.85°	0.79*	0.90'	0.97	1.00	0.99
	BART-sv-xalm-s	0.80°	0.80°	0.90'	0.99	1.01	1.00	0.99	0.97	0.98	1.02	1.01	1.03
	BART-hom-u-m	0.82*	0.84°	0.90'	0.95'	0.97	0.99	1.01	1.04	1.04	1.05	1.06	1.05
Pre Covid	GP-sv-xalm-s	0.73*	0.72*	0.86'	0.87*	0.91*	0.94'	0.89°	0.87*	0.92'	0.91'	0.92'	0.93
	GP-sv-xalm-b	0.74*	0.79*	0.90'	0.89*	0.93°	0.96	0.93	0.90'	0.98	0.98	1.00	1.01
	BLR-sv-xalm-m	0.70*	0.72*	0.86°	0.90'	0.93	0.98	0.89°	0.82*	0.93'	0.93	0.94	0.96
	BLR-sv-xalm-b	0.68*	0.74*	0.88'	0.90°	0.92'	1.00	0.91'	0.84*	0.96	0.99	0.99	1.01
	BART-sv-xalm-s	0.76*	0.76*	0.92	0.92'	0.97	0.97	0.99	0.99	0.99	1.00	1.00	1.01
	BART-hom-u-m	0.80*	0.83*	0.91°	0.91°	0.94'	0.95'	1.03	1.03	1.03	1.00	1.00	0.99
Recession	GP-sv-xalm-s	0.54'	0.53'	0.65'	0.79'	0.90'	0.94	1.00	0.92	0.87	0.87	0.88	0.86
	GP-sv-xalm-b	0.62'	0.68'	0.79	0.91	0.95	0.95	0.94	0.95	1.00	1.00	0.97	0.89
	BLR-sv-xalm-m	0.55'	0.58	0.76	0.88	0.92	1.00	1.02	0.75	0.89	0.77	0.69	0.71
	BLR-sv-xalm-b	0.54'	0.68	0.84	0.96	0.94	1.10	0.90	0.70	0.92	0.86	0.64	0.66
	BART-sv-xalm-s	0.61'	0.60	0.72'	0.78'	0.99	0.88	1.29	1.20	0.97	1.12	1.11	0.85
	BART-hom-u-m	0.76'	0.84	0.88	0.95	1.01	1.03	0.99	0.91	0.83	0.86	0.84	0.92

h

(b) CRPS-R

		GDPC1						GDPCTPI					
		0	1/3	2/3	1	4/3	5/3	0	1/3	2/3	1	4/3	5/3
Full	GP-sv-xalm-s	0.70°	0.67'	0.80	0.89*	0.91°	0.92°	0.84*	0.86*	0.85*	0.83*	0.84*	0.87°
	GP-sv-xalm-b	0.69°	0.71'	0.81	0.89*	0.91*	0.93°	0.82°	0.79*	0.78*	0.86°	0.87*	0.89°
	BLR-sv-xalm-m	0.61°	0.83	0.69	1.01	1.06	0.98	0.79*	0.81*	0.83*	0.87	0.92	0.86°
	BLR-sv-xalm-b	0.57°	0.77	0.71	0.94°	0.98	0.98	0.78*	0.76*	0.83*	0.87°	0.94	0.89°
	BART-sv-xalm-s	0.76'	0.74°	0.85	0.97	0.99	0.99	0.88°	0.89°	0.90'	0.90'	0.91'	0.92
	BART-hom-u-m	0.77'	0.77'	0.84'	0.90°	0.94'	0.98	0.93	0.95	0.96	0.97	0.97	0.96
Pre Covid	GP-sv-xalm-s	0.70*	0.72*	0.85°	0.86*	0.91°	0.93'	0.76*	0.76*	0.80*	0.77*	0.79*	0.82*
	GP-sv-xalm-b	0.72*	0.79*	0.89°	0.87*	0.91*	0.93*	0.85°	0.79*	0.84*	0.87°	0.88°	0.89°
	BLR-sv-xalm-m	0.71*	0.73*	0.85*	0.90°	0.96	0.98	0.81*	0.77*	0.83*	0.78*	0.79*	0.81*
	BLR-sv-xalm-b	0.70*	0.74*	0.88*	0.88*	0.93°	0.98	0.81*	0.77*	0.85*	0.85°	0.89	0.88°
	BART-sv-xalm-s	0.74*	0.73*	0.90'	0.92'	0.96	0.97	0.86*	0.87°	0.89°	0.87°	0.88°	0.90'
	BART-hom-u-m	0.80*	0.81*	0.90°	0.91°	0.95'	0.97	0.96	0.94	0.95	0.90'	0.91'	0.91'
Recession	GP-sv-xalm-s	0.47*	0.49*	0.65*	0.71*	0.80*	0.84°	1.06	0.92	0.92	0.85	0.88	0.87
	GP-sv-xalm-b	0.53*	0.60°	0.75°	0.81*	0.87°	0.86°	1.10	1.11	0.95	1.03	0.99	0.92
	BLR-sv-xalm-m	0.53°	0.59'	0.69°	0.73*	0.78*	0.84*	1.08	0.79	0.94	0.74'	0.72'	0.73'
	BLR-sv-xalm-b	0.50*	0.62°	0.76°	0.82*	0.86°	0.96	0.91	0.74	0.87	0.65'	0.70	0.67
	BART-sv-xalm-s	0.54*	0.56°	0.71°	0.74*	0.91°	0.83*	1.18	1.10	1.11	1.10	1.12	0.92
	BART-hom-u-m	0.64*	0.67*	0.79°	0.85°	0.91'	0.92°	1.08	1.04	1.02	0.93	0.94	0.96

h

Fig. 4: Predictive losses for selected specifications relative to the benchmark $AR(P_L)$ -model. Notes: Levels of statistical significance $\{5, 1, 0.1\}\%$ for a DM-test of equal predictive accuracy are indicated with $\{', \circ, *\}$. Best-performing specification by horizon in bold.

performs well in recessions in now- and forecasting downside risks of GDP growth, and this is also one of the few instances when BART can also improve significantly upon our benchmark.

Looking at the right tail forecasts in the lower panels of Figure 4, patterns appear less clear, but several similarities to previous results can be observed. Again, *sv-xalm* always makes up the best-performing models. BLR performs relatively well in nowcasting GDP growth and inflation, however, GP specifications outperform it across several horizons, especially during the pre-Covid period. Given the economic relevance of the right tail of inflation (especially when compared to GDP growth), it is also worth pointing out that every single one of our model specifications improves upon the $AR(P_L)$ -benchmark, both for the pre-Covid and full sample.

4. CONCLUSIONS

This paper proposes Bayesian nonparametric methods to be used with MIDAS regressions. Specifically, we consider GP and BART as flexible alternatives to the penalized linear framework. Our models are also equipped with stochastic volatility, and they are further differentiated with respect to specifics about MIDAS weighting schemes.

The resulting specifications are applied to nowcast and forecast US real output growth and inflation in the GDP deflator in a large-scale out-of-sample exercise. The set of potential predictors features up to almost 120 variables for our evaluation period, which starts in the late 1980s. The new models are competitive and offer gains in predictive accuracy, for point, density and tail forecasts, in many cases.

REFERENCES

- ANDREOU E, GHYSELS E, AND KOURTELLOS A (2010), “Regression models with mixed sampling frequencies,” *Journal of Econometrics* **158**(2), 246–261.
- BABII A, GHYSELS E, AND STRIAUKAS J (2022), “Machine learning time series regressions with an application to nowcasting,” *Journal of Business & Economic Statistics* **40**(3), 1094–1106.
- BHATTACHARYA A, CHAKRABORTY A, AND MALICK BK (2016), “Fast sampling with Gaussian scale mixture priors in high-dimensional regression,” *Biometrika* **103**(4), 985–991.
- BREITUNG J, AND ROLING C (2015), “Forecasting inflation rates using daily data: A nonparametric MIDAS approach,” *Journal of Forecasting* **34**(7), 588–603.
- CARRIERO A, CLARK TE, AND MARCELLINO M (2015), “Realtime nowcasting with a Bayesian mixed frequency model with stochastic volatility,” *Journal of the Royal Statistical Society Series A: Statistics in Society* **178**(4), 837–862.
- (2022), “Nowcasting tail risk to economic activity at a weekly frequency,” *Journal of Applied Econometrics* **37**(5), 843–866.
- CARVALHO CM, POLSON NG, AND SCOTT JG (2010), “The horseshoe estimator for sparse signals,” *Biometrika* **97**(2), 465–480.
- CHIPMAN HA, GEORGE EI, AND MCCULLOCH RE (2010), “BART: Bayesian additive regression trees,” *The Annals of Applied Statistics* **4**(1), 266–298.
- CLARK TE, HUBER F, KOOP G, AND MARCELLINO M (2024a), “Forecasting US inflation using Bayesian nonparametric models,” *Annals of Applied Statistics* **in-press**.
- CLARK TE, HUBER F, KOOP G, MARCELLINO M, AND PFARRHOFFER M (2023), “Tail forecasting with multivariate bayesian additive regression trees,” *International Economic Review* **64**(3), 979–1022.
- (2024b), “Investigating Growth-at-Risk Using a Multicountry Non-parametric Quantile Factor Model,” *Journal of Business & Economic Statistics* **in-press**.
- FORONI C, MARCELLINO M, AND SCHUMACHER C (2015), “Unrestricted mixed data sampling (MIDAS): MIDAS regressions with unrestricted lag polynomials,” *Journal of the Royal Statistical Society: Series A (Statistics in Society)* **178**(1), 57–82.
- GHYSELS E (2016), “Macroeconomics and the reality of mixed frequency data,” *Journal of Econometrics* **193**(2), 294–314.
- GHYSELS E, MARCELLINO M, AND VALKANOV R (2024), *The econometric analysis of mixed frequency data sampling*, Cambridge: Cambridge University Press.
- GHYSELS E, SINKO A, AND VALKANOV R (2007), “MIDAS regressions: Further results and new directions,” *Econometric Reviews* **26**(1), 53–90.

- GIACOMINI R, AND KOMUNJER I (2005), "Evaluation and combination of conditional quantile forecasts," *Journal of Business & Economic Statistics* **23**(4), 416–431.
- GNEITING T, AND RAFTERY AE (2007), "Strictly proper scoring rules, prediction, and estimation," *Journal of the American statistical Association* **102**(477), 359–378.
- GNEITING T, AND RANJAN R (2011), "Comparing density forecasts using threshold-and quantile-weighted scoring rules," *Journal of Business & Economic Statistics* **29**(3), 411–422.
- HASTIE T, TIBSHIRANI R, AND FRIEDMAN J (2009), *The Elements of Statistical Learning*, NY: Springer New York, 2nd edition.
- HAUZENBERGER N, HUBER F, MARCELLINO M, AND PETZ N (2024), "Gaussian process vector autoregressions and macroeconomic uncertainty," *Journal of Business and Economic Statistics* **in press**.
- HUBER F, KOOP G, ONORANTE L, PFARRHOFER M, AND SCHREINER J (2023), "Nowcasting in a pandemic using non-parametric mixed frequency VARs," *Journal of Econometrics* **232**(1), 52–69.
- KASTNER G, AND FRÜHWIRTH-SCHNATTER S (2014), "Ancillarity-sufficiency interweaving strategy (ASIS) for boosting MCMC estimation of stochastic volatility models," *Computational Statistics & Data Analysis* **76**, 408–423.
- KOHNS D, AND POTJAGAILO G (2023), "Flexible Bayesian MIDAS: time-variation, group-shrinkage and sparsity," Staff Working Paper No. 1025, Bank of England.
- KOOP G (2003), *Bayesian econometrics*, Wiley.
- MARCELLINO M, AND PFARRHOFER M (2024), "Bayesian Nonparametric Methods for Macroeconomic Forecasting," in MP CLEMENTS, AND AB GALVAO (eds.) "Handbook of Macroeconomic Forecasting," Edward Elgar Publishing Ltd.
- MCCRACKEN M, AND NG S (2016), "FRED-MD: A monthly database for macroeconomic research," *Journal of Business & Economic Statistics* **34**(4), 574–589.
- (2020), "FRED-QD: A quarterly database for macroeconomic research," *NBER Working Paper* **26872**.
- MOGLIANI M, AND SIMONI A (2021), "Bayesian MIDAS penalized regressions: estimation, selection, and prediction," *Journal of Econometrics* **222**(1), 833–860.
- PETTENUZZO D, TIMMERMANN A, AND VALKANOV R (2016), "A MIDAS approach to modeling first and second moment dynamics," *Journal of Econometrics* **193**(2), 315–334.
- RODRIGUEZ A, AND PUGGIONI G (2010), "Mixed frequency models: Bayesian approaches to estimation and prediction," *International Journal of Forecasting* **26**(2), 293–311.
- WILLIAMS CK, AND RASMUSSEN CE (2006), *Gaussian processes for machine learning*, volume 2, Cambridge, MA, USA: MIT Press.

Online Appendix: Nowcasting with mixed frequency data using Gaussian processes

A.1. APPENDIX

Table A.1.1: Data description.

Code	Description	Trans.	Code	Description	Trans.
<i>Quarterly target variables</i>					
GDPGCI	Real GDP, 3 Decimal (Billions of Chained 2012 \$)	8	GDPCTPI	GDP: Chain-type Price Index (Index 2009=100)	8
<i>Monthly predictors</i>					
RPI	Real Personal Income	5	AMDMUOx	Unfilled Orders for Durable Goods	5
W875RX1	Real personal income ex transfer receipts	5	BUSINVx	Total Business Inventories	5
DPCERA3M086SBEA	Real personal consumption expenditures	5 x x	ISRATIOx	Total Business: Inventories to Sales Ratio	2
CMRMTSPLx	Real Manu. and Trade Industries Sales	5	M2SL	M2 Money Stock	6 x
RETAILx	Retail and Food Services Sales	5 x	M2REAL	Real M2 Money Stock	5
INDPRO	IP Index	5 x x	BUSLOANS	Commercial and Industrial Loans	6
IPFPNSS	IP: Final Products and Nonindustrial Supplies	5	REALLN	Real Estate Loans at All Commercial Banks	6
IPFINAL	IP: Final Products (Market Group)	5	NONREVSL	Total Nonrevolving Credit	6
IPCNGD	IP: Consumer Goods	5	CONSPI	Nonrevolving consumer credit to Personal Income	2
IPDCONGD	IP: Durable Consumer Goods	5	S&P 500	S&P's Common Stock Price Index: Composite	5 x x
IPNCONGD	IP: Nondurable Consumer Goods	5	S&P: indust	S&P's Common Stock Price Index: Industrials	5
IPBUSEQ	IP: Business Equipment	5	FEDFUNDS	Effective Federal Funds Rate	2 x x
IPMAT	IP: Materials	5	TB3MS	3-Month Treasury Bill:	2
IPDMAT	IP: Durable Materials	5	TB6MS	6-Month Treasury Bill:	2
IPNMAT	IP: Nondurable Materials	5	GS1	1-Year Treasury Rate	2
IPMANSICS	IP: Manufacturing (SIC)	5	GS5	5-Year Treasury Rate	2
IPBS1222s	IP: Residential Utilities	5	GS10	10-Year Treasury Rate	2 x x
IPFUELS	IP: Fuels	5	AAA	Moody's Seasoned Aaa Corporate Bond Yield	2
CUMFNS	Capacity Utilization: Manufacturing	2 x	BAA	Moody's Seasoned Baa Corporate Bond Yield	2
HWI	Help-Wanted Index for United States	2	COMPAPFFx	3-Month Commercial Paper Minus FEDFUNDS	1
HWIURATIO	Ratio of Help Wanted/No. Unemployed	2	TB3MFFM	3-Month Treasury C Minus FEDFUNDS	1
CLF16OV	Civilian Labor Force	5	TB6MFFM	6-Month Treasury C Minus FEDFUNDS	1
CE16OV	Civilian Employment	5 x	T1YFFM	1-Year Treasury C Minus FEDFUNDS	1
UNRATE	Civilian Unemployment Rate	2 x x	TSYFFM	5-Year Treasury C Minus FEDFUNDS	1
UEMPMEAN	Average Duration of Unemployment (Weeks)	2	T10YFFM	10-Year Treasury C Minus FEDFUNDS	1 x
UEMPLT5	Civilians Unemployed - Less Than 5 Weeks	5	AAAFFM	Moody's Aaa Corporate Bond Minus FEDFUNDS	1 x
UEMP5T014	Civilians Unemployed for 5-14 Weeks	5	BAAFFM	Moody's Baa Corporate Bond Minus FEDFUNDS	1 x x
UEMP15OV	Civilians Unemployed - 15 Weeks & Over	5	EXSZUSx	Switzerland / U.S. Foreign Exchange Rate	5
UEMP15T26	Civilians Unemployed for 15-26 Weeks	5	EXJPUSx	Japan / U.S. Foreign Exchange Rate	5
UEMP27OV	Civilians Unemployed for 27 Weeks and Over	5	EXUSUKx	U.S. / U.K. Foreign Exchange Rate	5
CLAIM5x	Initial Claims	5 x x	EXCAUSx	Canada / U.S. Foreign Exchange Rate	5
PAYEMS	All Employees: Total nonfarm	5 x x	WPSFD49207	PPI: Finished Goods	6
USGOOD	All Employees: Goods-Producing Industries	5	WPSFD49502	PPI: Finished Consumer Goods	6
CES1021000001	All Employees: Mining and Logging: Mining	5	WPSID61	PPI: Intermediate Materials	6
USCONS	All Employees: Construction	5	WPSID62	PPI: Crude Materials	6
MANEMP	All Employees: Manufacturing	5	OILPRICEx	Crude Oil, spliced WTI and Cushing	6 x
DMANEMP	All Employees: Durable goods	5	PPICMM	PPI: Metals and metal products:	6
NDMANEMP	All Employees: Nondurable goods	5	CPIAUCSL	CPI: All Items	6 x x
SRVPRD	All Employees: Service-Providing Industries	5	CPIAPPSL	CPI: Apparel	6
USTPU	All Employees: Trade, Transportation & Utilities	5	CPITRNSL	CPI: Transportation	6
USWTRADE	All Employees: Wholesale Trade	5	CPIMEDSL	CPI: Medical Care	6
USTRADE	All Employees: Retail Trade	5	CUSR0000SAC	CPI: Commodities	6
USFIRE	All Employees: Financial Activities	5	CUSR0000SAD	CPI: Durables	6
USGOVT	All Employees: Government	5	CUSR0000SA5	CPI: Services	6
CES0600000007	Avg Weekly Hours : Goods-Producing	1 x x	CPIULFSL	CPI: All Items Less Food	6
AWOTMAN	Avg Weekly Overtime Hours : Manufacturing	2	CUSR0000SA0L2	CPI: All items less shelter	6
AWHMAN	Avg Weekly Hours : Manufacturing	1 x	CUSR0000SA0L5	CPI: All items less medical care	6
HOUST	Housing Starts: Total New Privately Owned	4 x x	PCEPI	Personal Cons. Expend.: Chain Index	6 x
HOUSTNE	Housing Starts, Northeast	4	DDURRG3M086SBEA	Personal Cons. Exp: Durable goods	6
HOUSTMW	Housing Starts, Midwest	4	DNDGRG3M086SBEA	Personal Cons. Exp: Nondurable goods	6
HOUSTS	Housing Starts, South	4	DSERRG3M086SBEA	Personal Cons. Exp: Services	6
HOUSTW	Housing Starts, West	4	CES0600000008	Avg Hourly Earnings : Goods-Producing	6 x
PERMIT	New Private Housing Permits (SAAR)	4 x	CES2000000008	Avg Hourly Earnings : Construction	6
PERMITNE	New Private Housing Permits, Northeast (SAAR)	4	CES3000000008	Avg Hourly Earnings : Manufacturing	6
PERMITMW	New Private Housing Permits, Midwest (SAAR)	4	DTCOLNVHFNFM	Consumer Motor Vehicle Loans Outstanding	6
PERMITS	New Private Housing Permits, South (SAAR)	4	DTCTHFNFM	Total Consumer Loans and Leases Outstanding	6
PERMITW	New Private Housing Permits, West (SAAR)	4	INVEST	Securities in Bank Credit at All Commercial Banks	6
AMDMNOx	New Orders for Durable Goods	5	VIXCLSx	VIX	1

Notes: The column *Trans.* denotes the following data transformation for a series x : (1) no transformation; (2) Δx_t ; (3) $\Delta^2 x_t$; (4) $\log(x_t)$; (5) $\Delta \log(x_t)$; (6) $\Delta^2 \log(x_t)$; (7) $\Delta(x_t/x_{t-1} - 1)$; (8) $100 \times ((x_t/x_{t-1})^4 - 1)$. The columns S and M indicate that the variable is included in small or medium information set, respectively.